

Effect of magnetic dopant on the metallic conductance of polyacetylene at low temperature

T. Masui and T. Ishiguro

Department of Physics, Kyoto University, Kyoto 606-8502, Japan

J. Tsukamoto

Polymer Research Laboratory, Toray Industries Inc., Otsu 520-0842, Japan

(Received 19 May 1997; revised manuscript received 17 November 1997)

The low-temperature metallic conductance in FeCl_4^- - and ClO_4^- -doped polyacetylene has been studied with the aim to probe the conduction electron-dopant interaction. A different behavior ascribable to the magnetic moment at the dopant site was found below ~ 1 K under a magnetic field of less than ~ 1 T. The result is discussed with respect to the effect of scattering by localized spins at the FeCl_4^- site. The logarithmic temperature dependence and the negative magnetoresistance are examined in relation to spin scattering at the magnetic dopant and at the carbonyl basis, and to pseudospin scattering due to dynamic chain distortion. The effect of inhomogeneity is discussed also. [S0163-1829(98)00631-6]

I. INTRODUCTION

The metallic phase in doped polyacetylene has been revealed by the study of high electrical conductance with weak temperature dependence at very low temperature down to the mK region.¹⁻⁴ Since the length of a polyacetylene chain is of the order of 10^2 nm and is much less than the sample size,^{3,5} the metallic conductance in such a quasi-one-dimensional electronic system is not understandable unless the appreciable role of interchain transfer is taken into account in the conductance processes. In other words, provided that the chains are not bypassed through interchain transfer,⁶⁻⁸ the charged carriers are hindered from transferring between the polymer chains at the terminals.

The undoped polyacetylene with quasi-one-dimensional electronic structure is insulating due to the strong electron-lattice and electron-electron interaction.^{9,10} The conduction carriers are produced by doping. In this case the addition of dopants enlarges the interchain spacing and inevitably modifies the structure according to the size and shape of the dopants.^{11,12} The expansion may work to reduce the interchain interaction. Then we take into account the roles of the dopants in the interchain electron transfer. It has been thought that the dopants are inactive electronically because most of the dopant species have a closed-shell structure, and thereby do not play a dominant role in interchain transfer. However, Yamashiro *et al.* showed that an alkali-metal dopant with a closed shell can mediate the interchain electron transfer via the extended wave function ranging over several carbon atoms aligned in adjacent chains.¹³ The resultant electron transfer was estimated to be comparable to the electron transfer within the chain. Then it is interesting to study the effect of the dopant to the conduction process.

The characteristics of low-temperature metallic conductance have been studied extensively using I_3^- -doped or FeCl_4^- -doped polyacetylene.^{1,2,14,15} When the dopants are supplied into aligned polyacetylenes up to saturation point, a high level of electrical conductance, well exceeding 10^4 S/cm with very weak temperature dependence, is realized at the fresh state. However, since it is considered that the dop-

ing does not proceed uniformly, the resultant inhomogeneity brings about a mixture of metallic and nonmetallic parts depending on the degree of disorder and hinders us from applying a simple model to the behavior.^{8,16,17} The conductance is affected by localization caused by disorder.^{18,19} At very low temperature only the metallic phase with negligible contribution of the localization serves for conductance and the conducting system can be significantly simplified.

As a means to probe the conduction electron-dopant interaction serving metallic conductance, we have investigated the difference in the conductance between FeCl_4^- -doped and ClO_4^- -doped polyacetylene at very low temperature.^{3,15,20} In this study it is essential that FeCl_4^- -dopant possesses the localized magnetic moment of $\frac{5}{2}\mu_B$,²¹⁻²³ in contrast to the nonmagnetic ClO_4^- -dopant. Due to similarities in the dopant structure with tetrahedral symmetry, the resultant structures of the doped polyacetylene are expected to be similar^{11,24} and the effect of the structural difference is not significant. The difference observed under magnetic field can be ascribed to the effect of the carrier-dopant interaction under the influence of the localized moment. We recall that the effect of FeCl_4^- dopant to thermo-electric power above liquid-He temperature was studied in comparison with I_3^- -doped and AsF_6^- -doped.²⁵ However, the significance of the spin effect for the metallic conduction to be studied at very low temperature was not touched upon.

II. SAMPLE PREPARATION AND EXPERIMENTAL PROCEDURE

High-density polyacetylene films were synthesized in *cis*-form from six-nine grade acetylene monomer gas.²⁶ The catalyst used was tetrabutoxy titanium/triethyl aluminum [$\text{Ti}(\text{OBu})_4/\text{AlEt}_3$] with an Al/Ti ratio of 2.0, which was aged around 200°C for 30 min in decaline with a $\text{Ti}(\text{OBu})_4$ concentration of 1.0 mol/l. Polymerization was carried out for several hours at -70°C under ambient pressure. After polymerization, the film was washed in toluene and a hydrochloric acid/methanol solution. The prepared film had an av-

erage thickness of 5–10 μm and a shiny silvery luster. The film was uniaxially drawn by hand in air to a stretching ratio of 5–10, and preserved in sealed glass tube at $\sim -30^\circ\text{C}$ before it was used. For the conductivity measurement, the film was cut to the dimension of about $0.5\text{ mm} \times 10\text{ mm}$ with a thickness of $1\text{ }\mu\text{m}$ and was mounted on a Kapton film. Electrodes were formed by folding the film with Pt strips with a thickness of $10\text{ }\mu\text{m}$ to which carbon paste was added. The contact resistance was less than $10\text{ }\Omega$. The exposure time in air before doping was restricted with several minutes. The paste was dried in vacuum.

The FeCl_4^- doping was carried out by immersing the polyacetylene film in $0.04M$ FeCl_3 /nitromethane solution.^{22,23} During the course of the doping the conductivity was monitored, and an example of the conductance increase is shown in Fig. 1. After the doping procedure, the sample was washed with solvent five times and dried in vacuum for 2 h. Finally, the sample was taken out of the apparatus and quickly covered with Apiezon-*N* grease to prevent oxidation by air.

The ClO_4^- doping was carried out by immersing in solution, $0.1M$ $\text{Cu}(\text{ClO}_4)_2$ /acetonitrile.²⁷ The solution was prepared by dissolving $\text{Cu}(\text{ClO}_4)_2 \cdot 6\text{H}_2\text{O}$ with molecular sieves (hole size $3\text{ }\text{\AA}$, grain diameter $\frac{1}{8}$) in acetonitrile, and kept for 10 days to remove water. During ClO_4^- doping, the conductivity was not monitored in this case, because the solution was conductive, but it was evaluated with a calibration curve of conductivity versus doping time prepared by a series of dopings. After doping, the sample was washed, dried, and taken out similar to the method used in the case of FeCl_4^- doping. We found that the ClO_4^- -doped sample was influenced by air at a much faster rate than the FeCl_4^- -doped sample. The room-temperature resistivities on completing the preparation and at the start of the measurements are listed

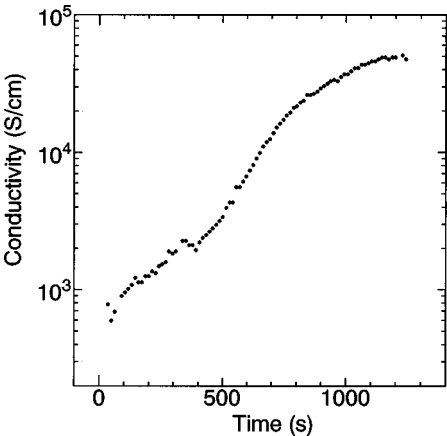


FIG. 1. The doping time dependence of conductivity for FeCl_4^- doping.

in Table I. Differences between the successive measurements can be ascribed to the room-temperature aging effect.

The measurements were carried out with a dilution refrigerator. The sample was mounted in an epoxy mixing chamber and immersed in ^3He - ^4He solution during measurements in order to ensure good thermal contact below 1 K . A RuO_2 resistance thermometer was used to monitor the sample temperature. The resistivity was measured by ac four-terminal method at frequencies of 12.5 or 23 Hz with an AC resistance bridge or a lock-in amplifier. The linearity of the measured resistance was checked intermittently at some temperatures. Magnetoresistance measurements were mainly carried out by sweeping the temperature under a constant field in order to avoid heating due to eddy current loss. The field was applied in the transverse direction. Previous works^{15,18,28,29}

TABLE I. Room-temperature resistivity of measured samples. The samples are numbered in sequence of measurement. For example, *F1* was measured after preparation, *F2* and *F3* were measured keeping *F1* at room temperature ~ 2 and ~ 8 days, respectively. The conductivity at room temperature is higher than those reported for $\text{S}(\text{CH})_x$ by two orders of magnitude (Ref. 19).

Dopant and sample code		Resistivity after doping ($10^{-5}\text{ }\Omega\text{ cm}$)	Resistivity before measurement ($10^{-5}\text{ }\Omega\text{ cm}$)	Thickness (μm)
ClO_4^-	<i>C1</i>	2.1	3.4	0.7
	<i>C2</i>	2.1	12	0.7
	<i>D1</i>	2.0	2.8	0.6
	<i>D2</i>	2.0	4.1	0.6
	<i>D3</i>	2.0	5.0	0.6
	<i>D4</i>	2.0	6.4	0.6
FeCl_4^-	<i>F1</i>	2.3	2.7	0.7
	<i>F2</i>	2.3	3.6	0.7
	<i>F3</i>	2.3	4.7	0.7
	<i>F4</i>	2.3	9.9	0.7
	<i>F5</i>	2.3	12	0.7
	<i>G1</i>	1.1	1.1	0.6

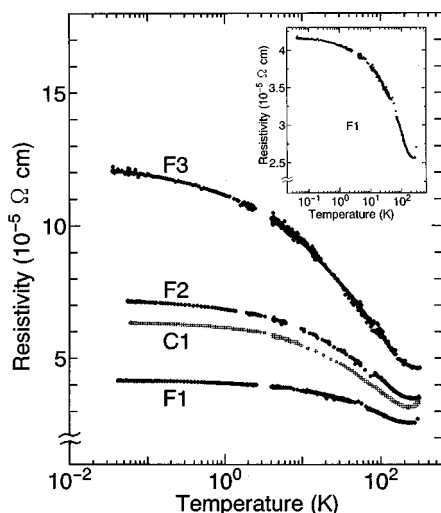


FIG. 2. The temperature dependencies of the resistivity of FeCl_4^- -doped (denoted with $F1$, $F2$, and $F3$) and ClO_4^- -doped ($C1$) polyacetylene. The specifications of the samples are given in Table I. The inset is given to magnify the resistive change for $F1$.

have shown that the direction of the field does not result in significant differences.

III. RESULTS

A. Temperature dependence of resistivity

The temperature dependence of the resistivity for a series of FeCl_4^- -doped samples denoted by F_n ($n=1,2,3$) is shown in Fig. 2. The freshest sample giving the lowest resistivity is denoted with $F1$, and those obtained after successive agings are denoted with $F2$ and $F3$. The characteristics of the samples are listed in Table I. The sample denoted with $C1$ is the freshest ClO_4^- -doped sample. The samples $F1$ and $C1$ were prepared from different parts of the same pristine film.

The resistivity of sample $F1$ increases gradually by cooling from 300 K to 40 mK. However, as displayed in the inset figure of Fig. 2, the temperature dependence is somewhat different for 300 to 200 K, 150 to 20 K, and below 1 K. The resistivity decreases on cooling from room temperature to 200 K, as reported in Ref. 15. The resistivity then increases with a high slope in the logarithmic temperature scale from 150 to 20 K, followed by a weak temperature dependence below 1 K. With increases in the room-temperature resistivity, as in $F2$ and $F3$, the resistivity minimum appearing near 200 K and above is suppressed and the slope of the resistive increase is enhanced in accordance with the previous report.¹⁵

Concerning the ClO_4^- -doped sample $C1$, the general features appear to be similar to the series of FeCl_4^- -doped samples, and the temperature dependence seems to be almost scaled with the room-temperature resistivity. We confirmed that with further aging, the nonmetallic behavior of the doped polyacetylene is enhanced due to strong localization by induced imperfections as has been reported in Refs. 15 and 18.

The samples $D1$ and $G1$ shown in Fig. 3 were also prepared from different parts of one pristine film. In order to see

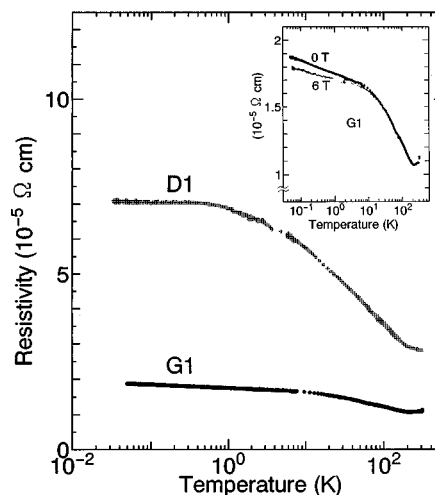


FIG. 3. The temperature dependencies of the resistivity of FeCl_4^- -doped ($G1$) and ClO_4^- -doped ($D1$) polyacetylenes. The samples were prepared from the same film, but this was different from the film used for samples $F1$ and $C1$. The specifications of the samples are given in Table I.

the dependence of the dopant species and to avoid the effects of differences ascribable to the pristine polyacetylene film, we doped different species to pieces of one film. The temperature dependence appearing above 10 K in Fig. 3 is similar to the cases shown in Fig. 2. On the other hand, the FeCl_4^- -doped sample $G1$ shows a logarithmic temperature dependence below 10 K, while the ClO_4^- -doped sample $D1$ exhibits almost temperature-independent resistivity below 1 K.

B. Effects of magnetic field

The magnetic field H dependence of the transverse magnetoconductance $\Delta\sigma(H)$ [$=\sigma(H)-\sigma(0)$, where $\sigma(H)$ is the conductivity under magnetic field H] is shown in Figs. 4 and 5, for the FeCl_4^- -doped and ClO_4^- -doped polyacetylene, respectively. The measurements were carried out by varying the temperature under a constant field, which was applied perpendicular to the current direction, in order to avoid heating due to eddy currents on the field sweep. The data are given as the magnetoconductance increment $\Delta\sigma(H)$ ($=[\rho(0)-\rho(H)]/\rho(0)^2$, where $\rho(H)$ is the resistivity). The observed magnetoresistance is negative. $\Delta\sigma(H)$ increases with H , with a larger increasing ratio below 1 T than above 2 T as shown in Figs. 4(a) and 4(c) for $F1$ and $G1$, respectively. With increases in the resistivity due to aging, the low-field increment is suppressed as shown in Fig. 4(b). With regard to the temperature dependence, in the case of the FeCl_4^- -doped sample, the value of $\Delta\sigma(H)$ continues to increase by cooling down to 40 mK.

In the case of the ClO_4^- -doped sample shown in Fig. 5, the $\Delta\sigma(H)$ increases with H , but the rise in the low-field region is not so obvious as in the case of the FeCl_4^- -doped sample. It is noteworthy that $\Delta\sigma(H)$ is almost temperature independent in the region below 1 K, in contrast to the case for the FeCl_4^- -doped samples, although $\Delta\sigma(H)$ decreases when heated above 1 K as shown in Fig. 5(b).

Here we discuss the relationship between the present results and the reported results of the low-temperature magne-

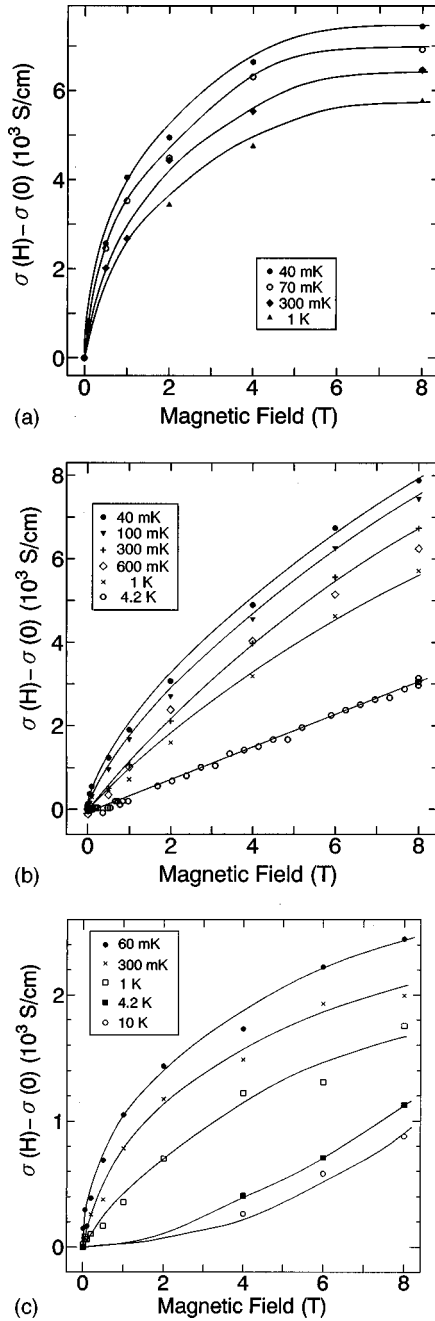


FIG. 4. The magnetic field dependence of the transverse magnetoconductance $\sigma(H) - \sigma(0)$ for FeCl_4^- -doped samples *F1*, *F3*, and *G1* in (a), (b), and (c), respectively. Lines are a guide for the eyes.

toresistance in I_3^- -doped highly conducting polyacetylene.²⁹ In the previous report, the magnetoresistance measurements were carried out up to 14.5 T in the temperature region above 0.55 K. The magnetoresistance for the most conductive sample (denoted sample *D* in Ref. 29) becomes negative and almost proportional to the magnetic-field. The measurement carried out down to 0.55 K under the longitudinal magnetic-field configuration shows that the magnetoconductance increment $\Delta\sigma(H)$ becomes insensitive below 0.9 K, which is consistent with the ClO_4^- -doped sample in the present study. The difference between the transverse and the longitudinal configurations is characterized by the enhancement in the former by a factor of ~ 2 .

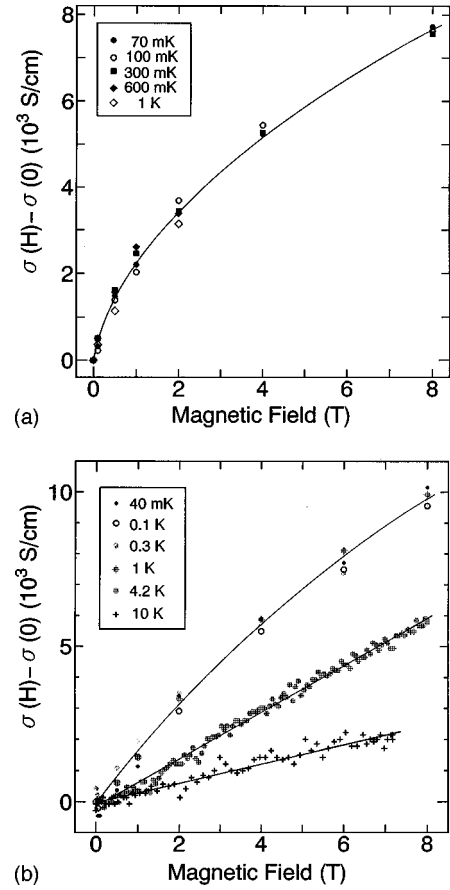


FIG. 5. The magnetic field dependence of the transverse magnetoconductance $\sigma(H) - \sigma(0)$ for ClO_4^- -doped samples *C1* and *D1* in (a) and (b), respectively. Lines are a guide for the eyes.

IV. DISCUSSION

A. Inhomogeneous structure

The doped polyacetylene samples adopted in this study were refined ones, as evidenced by a conductivity well exceeding 10^4 S/cm at room temperature. The doping up to the saturation level can minimize inhomogeneous dopant distribution. Even in this case, however, inhomogeneity cannot be ruled out, due to the higher-order structure characterized as assembly of fibrils with ~ 5 nm diameter.³

It is remarkable that bond alternation was observed through the infrared and the Raman spectra even in the heavily doped polyacetylene with metallic conductance.^{30,31} Provided that the material is uniform, this observation may mean the presence of an anomalous phase in which the bond alternation accompanied with an energy gap coexists with the metallic state possessing the finite density of states at the Fermi level.³² However, because the samples consist of polymer chains of higher-order structure, even in highly conductive polyacetylene, there is no reason to assert that the system should be homogeneous. A possibility that the central and terminal parts of the chains have different electronic structures cannot be ruled out. In other words, even when a central portion of the chain serves the metallic conduction, a terminal part of the chain may still be nonmetallic with a bond-alternating structure. This supports the idea that the metallic parts and the bond alternation coexist in a spatially separated fashion in the chain.

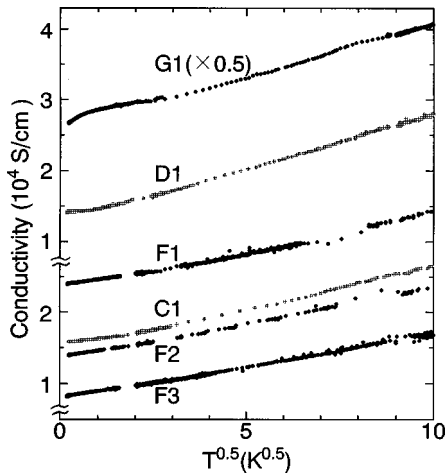


FIG. 6. The temperature (T) dependencies of the conductivity plotted versus $T^{0.5}$.

The residual conductance at very low temperatures, typically below 1 K, is considered to represent the nature of metallic portions connected bypassing the nonmetallic parts: the observation of the metallic conductance proves the existence of a genuine metallic phase, in the sense that carriers can be excited with infinitesimally small energy. Recently, the inhomogeneous coexistence of different electronic phases has been recognized in doped polypyrroles and polyanilines.^{33–35} Their metallic conductance at very low temperatures is ascribed to percolation through the metallic portions.

Prior to discussion of the metallic nature, we try to describe the temperature dependence of the conductivity in terms of weak localization.^{36,37} For this purpose, the conductivity is plotted against $T^{0.5}$ as shown in Fig. 6, while its increment by the magnetic field is plotted against $H^{0.5}$ in Fig. 7. Then we find that the relationship expected for the weak localization is not fully satisfied in the low-temperature side. We remember that the general feature from 100 to 1 K can be represented fairly well on the basis of the localization model modified by taking into account the low dimensionality.²⁹

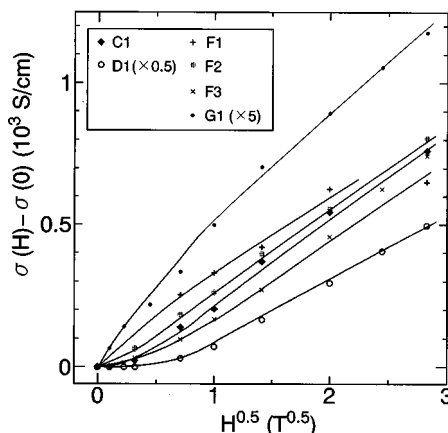


FIG. 7. The magnetic field (H) dependencies of the magnetoconductance [$\sigma(H) - \sigma(0)$] versus $H^{0.5}$ at 100 mK. Lines are a guide for the eyes.

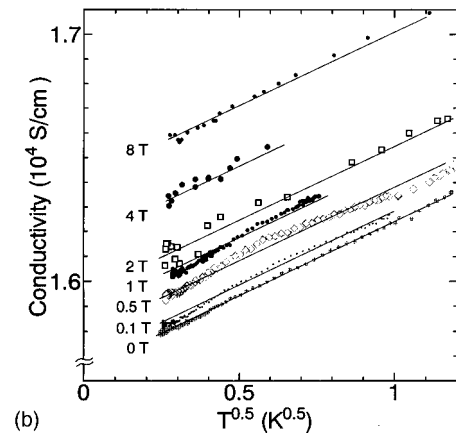
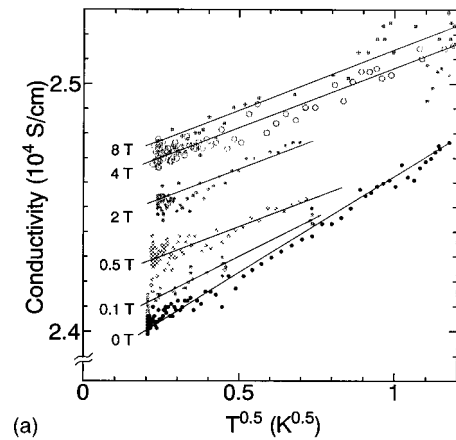


FIG. 8. The temperature dependence of conductivity under magnetic fields. (a) and (b) represent results for samples $F1$ and $C1$, respectively. Lines are a guide for the eyes.

B. Effect of spin scattering

The magnetoconductance increment $\Delta\sigma(H)$ for the ClO_4^- -doped samples is rather insensitive to temperatures below 1 K as shown in Figs. 5(a) and 5(b), in accordance with the I_3^- -doped polyacetylene.²⁹ On the other hand, $\Delta\sigma(H)$ for FeCl_4^- -doped samples continues to increase due to cooling below 1 K, as displayed in Figs. 4(a), 4(b) and 4(c). The difference can be seen alternatively if we plot the temperature dependence below 1 K, as shown in Figs. 8(a) and 8(b). The slopes in the temperature dependence below 1 K for the FeCl_4^- -doped samples change with fields up to 1 T [Fig. 8(a)], while the slopes for the ClO_4^- -doped samples are rather independent of the magnetic field [Fig. 8(b)]. We ascribe the $\Delta\sigma(H)$ below 1 K for the FeCl_4^- -doped samples to the role of the localized magnetic moment as follows.

The electron spin resonance (ESR) measurement carried out for a part of sample $G1$ indicated the presence of localized spins in the FeCl_4^- -doped samples. The signal was seen at $g \sim 2$, with the peak-to-peak width of about 500 Oe, which can be partly ascribed to the orientational averaging of the anisotropic fine structure coming from the Fe^{3+} ions.³⁸ The signal coming from conduction electrons could not be extracted. Figure 9 shows the spin susceptibility as a function of inverse temperature. The temperature dependence can be represented roughly as a sum of Curie and Pauli-like parts, indicating that the localized paramagnetic spins exist down to low temperature. By comparing the coefficient of the Cu-

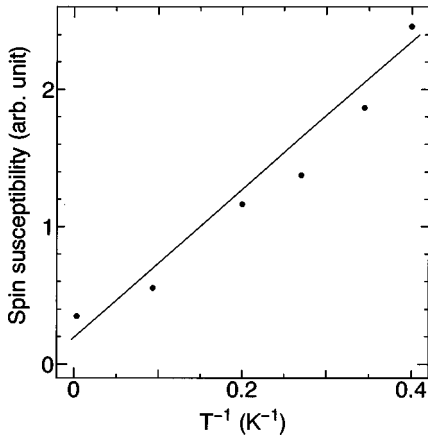


FIG. 9. The spin susceptibility of sample G1, obtained from ESR measurement. The line is a guide for the eyes.

rie part with the standard sample (DPPH), we obtain spin of $\sim 3.4\mu_B$ per dopant. The reason for getting the larger value compared to $\frac{5}{2}\mu_B$ for Fe^{3+} is not known but this means that the localized d orbitals are not hybridized with π electrons due to the spatial separation of the Fe^{3+} ion from the polyacetylene chain by holding Cl ion between them. It is worthy to note that the Zeeman splitting energy under 1 T corresponds to 1.4 K when $g=2$. It is suggestive that the difference in the magnetic field dependence between the FeCl_4^- - and the ClO_4^- -doped samples appears below ~ 1 K. The coincidence with regard to the ranges of the field and the temperature implies that the electrons interact with the localized spin below ~ 1 T for the FeCl_4^- -doped samples. The enhancement of $\Delta\sigma(H)$ by the magnetic field can be understood by considering the suppression of spin scattering due to the spin polarization by a magnetic field.

Assuming that the present system can be modeled by a metal with localized magnetic moments, the s - d interaction model of an electron with localized spin brings about the resistivity in the Born approximation as

$$R_B = \frac{3}{2} \frac{m\pi V c}{zNe^2\hbar} \frac{J^2}{\epsilon_F} S(S+1), \quad (1)$$

where m is the effective electron mass, zN is the number of conduction electrons, c is the concentration of impurity atoms, V is the volume of the system, S is the quantum number for the spin at the impurity site, J is the exchange integral, and ϵ_F is the Fermi energy.³⁹ The second-order Born approximation provides the Kondo scattering. In the present case with $S \cong \frac{5}{2}$, however, the applicability of the results based upon the s - d model is not guaranteed due to complexity related to the orbital degeneracy. Nevertheless, when we assume that the suppression of the spin scattering above ~ 1 T is due to spin polarization by the Zeeman effect, J^2/ϵ_F is given as 2×10^{-4} eV by $R_B = 1/\Delta\sigma$ at $H=1$ T. It is predicted that the magnetoresistance at sufficiently small field is proportional to the square of the magnetization, that is, proportional to H^2 . This tendency is found in the experimental results, although we should note that the effect of electron interaction in weakly disordered metallic systems also provides H^2 dependence.³⁷

It is noteworthy that the spin concentration reaches 0.1 per CH in the present system. In this situation, the interaction between the localized spins, the Ruderman-Kittel-Kasuya-Yoshida (RKKY) interaction via conduction carriers, may work, resulting in the suppression of spin scattering at low temperatures. In the polyacetylene with inherent quasi-one-dimensionality, the screening effect can be reduced and the RKKY interaction becomes so weak as not to form a spin-glass state. On the other hand, the magnetic-field dependence appearing above ~ 1 T is observed not only in FeCl_4^- -doped but also in ClO_4^- -doped samples, implying that it cannot be ascribed to the localized spins as will be discussed in Sec. IV E.

C. Effect of dopant on carrier transport

On considering the conduction electron-dopant interaction, we have to take into account the effect of the mixing of the wave function of dopants and that of conduction electron as well as the influence to the potential field. The charge transfer between dopants and polyacetylene chains notably modifies the conduction band as demonstrated for alkali-metal-doped polyacetylene.⁴⁰ With regard to FeCl_4^- and ClO_4^- , possessing the similar structure, the degree of the charge transfer is at the same level. For the case of FeCl_4^- , the central Fe^{3+} interacts with CH chains, holding Cl^- between them, and the direct mixing of the wave function of Fe^{3+} to that of conduction band is considered to be weak. Therefore, although we cannot thoroughly rule out a possibility of spin scattering for conduction electron in CH chain via the direct mixing, it is probable that the conduction carrier gets close to the Fe^{3+} site and are scattered by the localized spins.

On the other hand, it is noteworthy to see the results in the aged sample. The resistive increase by aging is ascribed to induced disorder in CH chains rather than dopant sites, because the aging effect is found in general, irrespective of dopant species. As shown in Figs. 10(a) and 10(b), the magnetoconductance appearing below 1 T remains for the FeCl_4^- -doped as in the case for the fresh sample. This is understandable if we can consider that an interchain transfer path involving the dopant that is less affected by aging serves to the conductance.

D. Magnetoresistance in aged samples

As aging progresses, the metallic percolation path for conduction is narrowed. The sign of magnetoresistance changes from negative to positive with aging.^{18,29,41} In the case of I_3^- and FeCl_4^- -doped polyacetylene, the dependence above 0.6 K was well explained by variable range hopping in a system with intrastate Coulomb correlation.⁴² Under a magnetic field, the spins of carriers tend to orient in the same direction. As a result, since the occupation of one site by two spins of the same orientation is inhibited, the hopping conduction is suppressed, resulting in the positive magnetoresistance exhibiting a saturating behavior at high magnetic field. In this case, the appearance of the resistivity maximum is determined by the influence of Zeeman energy on the localization. It is also dominated by the difference

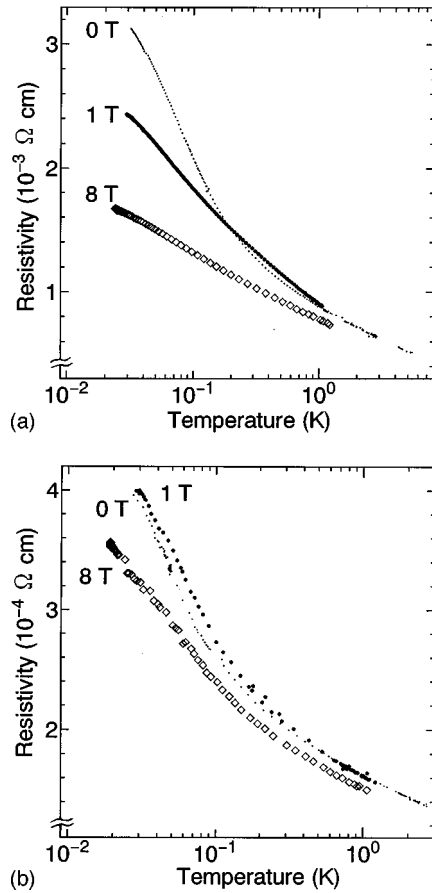


FIG. 10. The temperature dependence of resistivity for aged samples under magnetic field. (a) and (b) represent results for samples *F4* and *D2*, respectively.

between the Fermi energy and the mobility edge. In FeCl_4^- -doped samples, the carriers are delocalized by the Zeeman energy, but this is not the case in I_3^- -doped samples.⁴¹ It should be noted that the magnetoresistance described here can be ascribed to the carrier hopping among the localized sites in the CH chain. This contrasts to the effect of the spin scattering discussed in Sec. IV C.

The magnetoconductance of the aged samples such as *F5* and *D4* is presented in Figs. 11(a) and 11(b), respectively. In the ClO_4^- -doped case (sample *D4*), the feature is very similar to that of the I_3^- -doped case. In the FeCl_4^- -doped case (sample *F5*), however, the tendency above ~ 0.6 K is similar to that reported in Ref. 41, but a new feature is seen below 0.6 K. The conductance minimum vanishes and positive magnetoconductance emerges. The increase in conductance is further enhanced at low field below ~ 1 T being consistent with results shown in Figs. 10(a) and 10(b). This is in accordance with the effects of spin scattering observed in a fresh sample, implying that some conduction paths remain at very low temperature in the aged sample.

E. Logarithmic dependence

The temperature dependence of the resistivity in the doped metallic polyacetylene is characterized by a component proportional to $\ln T$,^{43,44} although it may be separated

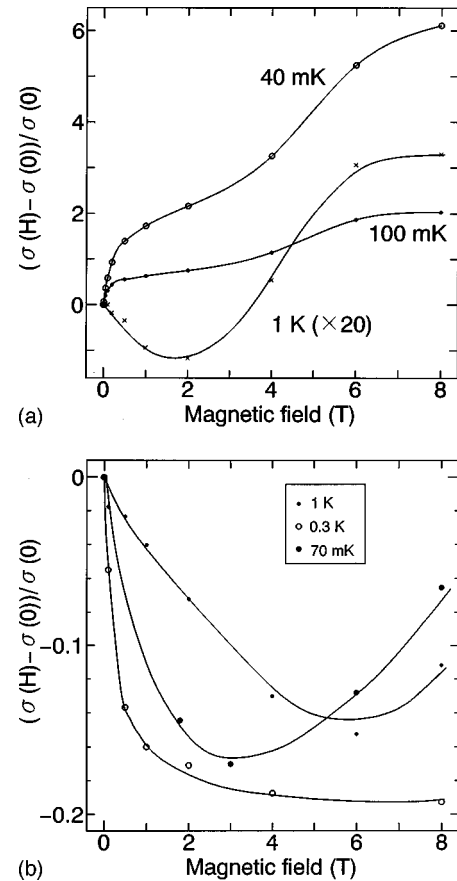


FIG. 11. The magnetic-field dependence of conductance for aged samples. (a) and (b) represent results for *F5* and *D4*. Lines are a guide for the eyes.

into two parts, depending on temperature, from 150 to 20 K and below 1 K. By aging at room temperature, the temperature dependence appearing in the higher-temperature region is smoothly expanded to lower temperatures, and the rate of the temperature dependence is enhanced.

To explain the logarithmic temperature dependence in conducting polymers, there have been three proposals as follows. The first describes this temperature dependence as the effect of localized magnetic moment as in the case of dilute magnetic alloys.³⁹ The second points to the effects of carbonyl defects formed in polyacetylene chains, which have lone electrons and act as an Anderson U impurity with a spin degree of freedom.⁴⁵ The third explanation suggests that the effect of a two-level system associates with disorder in weak interchain binding among polymers, as in the case of amorphous metals.^{46,47}

With regard to the effects of localized magnetic moment at Fe^{3+} , we found that the metallic conductance in the FeCl_4^- -doped samples showed more variation with temperature than that of ClO_4^- -doped samples, as demonstrated in Fig. 2 with samples *F1* and *C1*, and also in Fig. 3 with samples *G1* and *D1*. We attempted to measure ClO_4^- -doped samples in their fresh state, but we could not suppress the aging prior to our measurements, as evidenced by the higher room-temperature resistivity compared to the FeCl_4^- -doped samples. Since the *F1* and *C1* samples were prepared from the same film, the pristine structure of the polyacetylene film was identical. The difference in the resis-

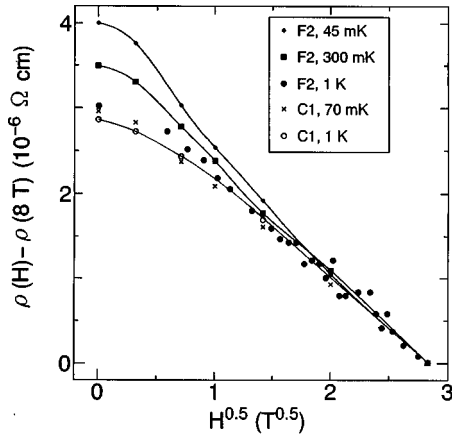


FIG. 12. The magnetic-field dependencies of $\rho(H) - \rho(8 \text{ T})$ for samples C1 and F2, at different temperatures. Lines are a guide for the eyes.

tivity can be ascribed to the difference in the dopant species and the defect structure. The systematic variation of the temperature dependence from sample F1 to F3 and the similar dependence of sample C1 displayed in Fig. 2 supports this view. In this case, it is noteworthy that the variation in sample F1 is larger than that in sample C1 below 1 K, where the metallic conductance dominates. In order to show that the resistivity of sample F2 have a component proportional to $\ln T$ in contrast to that of C1, we processed the data in the following way. First the magnetic-field dependence of $\rho(H) - \rho(8 \text{ T})$ for sample F2 and C1 at different temperature was derived as shown in Fig. 12. This enables us to extract the effect of the spin scattering at low fields. (The magnetic field was scaled with \sqrt{H} , since the field dependence above 1 T can be represented in a simple fashion.) It is noteworthy that $\rho(H) - \rho(8 \text{ T})$ for sample F2 varies with temperature in the low-field region while that for sample C1 is rather independent of temperature. Then we get the $\Delta\rho(T)$ at $H=0$ for sample F2 is proportional to $\ln T$ as shown in Fig. 13.

The logarithmic temperature dependence seems to be consistent with differences in the magnetic-field dependence as discussed in Sec. IV B. In this case we are tempted to relate

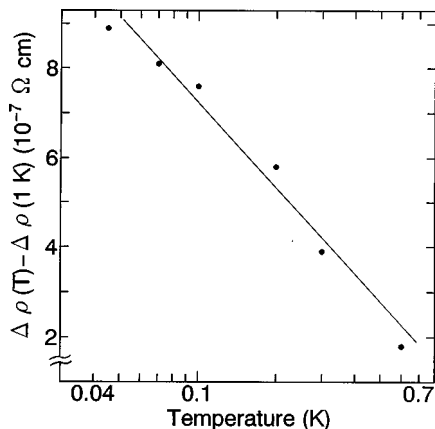


FIG. 13. The temperature dependence of $\Delta\rho(T) - \Delta\rho(1 \text{ K})$, where $\Delta\rho(T) = \rho(0) - \rho(8 \text{ T})$ for sample F2. The line is a guide for the eyes.

the result to the logarithmic temperature dependence derived from the second Born approximation. However, we should note that in the present case, the theoretical result giving the logarithmic temperature dependence of the resistivity cannot be applied directly because the localized moment has $\frac{5}{2}$ spin and can have orbital degeneracy. In this respect, although the influence of the magnetic dopant cannot be directly interpreted in terms of the Kondo theory, the temperature dependence shown in Fig. 13 is considered to be related to something similar to that. We also point out that because the d orbital is not fully mixed with the π electrons, it is difficult to form the hybridized state.

In the case of the carbonyl impurity that can appear in both FeCl_4^- -doped and ClO_4^- -doped samples due to aging in atmosphere, the localized states are buried in the conduction path and hence can be hybridized with the π electrons as described by the Anderson model. Cruz *et al.* have claimed that in this case Kondo resonance can appear, resulting in a unitary state at low temperatures where the logarithmic temperature dependence tends to be suppressed. In order to check the validity of the model, we refer to the magnetoresistance measured up to 8 T. As shown in Figs. 10(a) and 10(b), the logarithmic dependence in aged samples such as F4 and D2, is not suppressed even under high magnetic field, which is enough to polarize the localized spins. This implies that the scattering is not of magnetic origin.

The third model related to the structural freedom due to distortion in the loosely bound polymer chains can be independent of the magnetic field. We note that the effect may be subtle since the scattering giving the logarithmic temperature dependence is ranked to a higher-order process.⁴⁷ Previously, Kaneko *et al.*⁴⁸ have ascribed the temperature dependence in the intermediate temperature region to the localization effect in the restricted dimensional system. One problem to be solved, however, is that the high field reaching 10 T still strongly influences the conductance as shown in Fig. 12. With regard to the magnetic-field dependence of the metallic conductance appearing below $\sim 1 \text{ K}$ in FeCl_4^- -doped fresh samples such as F1 and G1, we cannot dismiss the magnetic-field dependence appearing above $\sim 1 \text{ T}$. Since the similar magnetic-field dependence is seen as well in the ClO_4^- -doped samples, this cannot be ascribed to the magnetic origin but may be related to the electronic structure appearing at the boundary between the metallic and nonmetallic parts.

V. SUMMARY

The electrical conductance of heavily FeCl_4^- - and ClO_4^- -doped polyacetylene shows similar temperature dependence from room temperature down to the mK region, except for differences found in the low-temperature magnetoresistance below $\sim 1 \text{ T}$ and the somewhat enhanced logarithmic temperature dependence of the resistivity in the former.

The difference in the magnetoresistance can be ascribed to spin scattering by the magnetic dopant. The enhanced magnetic-field effect in aged samples implies that the conductance along the chain is suppressed by disorder presumably due to oxidation of polyacetylene, while the effect of

the spin scattering is less influenced. These facts suggest that the carriers can transfer via the dopant site in interchain transfer process.

The logarithmic temperature dependence observed generally in heavily doped polyacetylene is examined in relation to spin scattering at the carbonyl defect, which is formed by oxidation and predicted to work as Anderson U impurity, and pseudospin scattering through the dynamic distortion of polymer chains. The influence of the magnetic field up to more than 10 T suggests that the spin scattering cannot be the origin of the logarithmic temperature dependence, since it is expected to be saturated by polarization at rather low

field. As the origin we cannot rule out the effects of localization in an inhomogeneously disordered system and the effect of the electronic state varying between the metallic and nonmetallic regions at their spatial boundary.

ACKNOWLEDGMENTS

This work was supported by a Grant-in-Aid for Scientific Research from the Ministry of Education, Science, Sports, and Culture and by the Proposal-Based Advanced Industrial Technology Research and Development program from NEDO.

- ¹C. M. Gould, D. M. Bates, H. M. Bozler, A. J. Heeger, M. A. Druy, and A. G. MacDiarmid, *Phys. Rev. B* **23**, 6820 (1981).
- ²H. Naarmann and N. Theophilou, *Synth. Met.* **22**, 1 (1987).
- ³J. Tsukamoto, *Adv. Phys.* **41**, 509 (1992).
- ⁴T. Ishiguro, H. Kaneko, J. P. Pouget, and J. Tsukamoto, *Synth. Met.* **69**, 37 (1995), and references therein.
- ⁵J. C. W. Chien, *Polyacetylene* (Academic Press, New York, 1984), p. 50.
- ⁶Z. H. Wang, C. Li, E. M. Scherr, A. G. MacDiarmid, and A. J. Epstein, *Phys. Rev. Lett.* **66**, 1745 (1991).
- ⁷V. N. Prigodin and K. B. Efetov, *Phys. Rev. Lett.* **70**, 2932 (1993).
- ⁸J. Joo, G. Du, V. N. Prigodin, J. Tsukamoto, and A. J. Epstein, *Phys. Rev. B* **52**, 8060 (1995).
- ⁹H. Fukutome and M. Sasai, *Prog. Theor. Phys.* **67**, 41 (1982).
- ¹⁰A. J. Heeger, S. Kivelson, J. R. Schrieffer, and W. P. Su, *Rev. Mod. Phys.* **60**, 781 (1988).
- ¹¹J. P. Pouget, A. Pron, A. Murasik, D. Billaud, J. C. Pouxviel, P. Robin, I. Kulszewicz, D. Begin, J. J. Demai, and S. Lefrant, *Solid State Commun.* **57**, 297 (1986).
- ¹²N. S. Murthy, L. W. Shacklette, and R. H. Baughman, *Solid State Commun.* **72**, 267 (1989).
- ¹³A. Yamashiro, A. Ikawa, and H. Fukutome, *Synth. Met.* **69**, 645 (1995); **74**, 29 (1995).
- ¹⁴Y. W. Park, C. Park, Y. S. Lee, C. O. Yoon, H. Shirakawa, Y. Suezaki, and K. Akagi, *Solid State Commun.* **65**, 147 (1988).
- ¹⁵H. Kaneko and T. Ishiguro, *Synth. Met.* **65**, 141 (1994), and references therein.
- ¹⁶A. J. Epstein, H. Rommelmann, M. A. Druy, A. J. Heeger, and A. G. MacDiarmid, *Solid State Commun.* **38**, 683 (1981).
- ¹⁷Y. Tomkiewicz, T. D. Schultz, H. B. Brom, A. R. Taranko, T. C. Clarke, and G. B. Street, *Phys. Rev. B* **24**, 4348 (1981).
- ¹⁸H. Kaneko, T. Ishiguro, J. Tsukamoto, and A. Takahashi, *J. Phys. Soc. Jpn.* **62**, 3621 (1993).
- ¹⁹A. J. Epstein, R. W. Biglow, H. Rommelmann, H. W. Gibson, R. J. Weagley, A. Feldblum, D. B. Tanner, J. P. Pouget, J. C. Pouxviel, R. Comes, P. Robin, and S. Kivelson, *Mol. Cryst. Liq. Cryst.* **117**, 147 (1985).
- ²⁰T. Miyamae, T. Mori, K. Seki, and J. Tanaka, *Bull. Chem. Soc. Jpn.* **68**, 803 (1995).
- ²¹Y. W. Park, J. C. Woo, K. H. Yoo, W. K. Han, C. H. Choi, T. Kobayashi, and H. Shirakawa, *Solid State Commun.* **46**, 731 (1983).
- ²²H. Kuroda, I. Ikemoto, K. Asakura, H. Ishii, H. Shirakawa, T. Kobayashi, H. Oyanagi, and T. Matsushita, *Solid State Commun.* **46**, 235 (1983).
- ²³E. K. Sichel, M. F. Rubner, J. Georger, Jr., G. C. Papaefthymiou, S. Ofer, and R. B. Frankel, *Phys. Rev. B* **28**, 6589 (1983).
- ²⁴S. Flandrois, A. Boukhari, A. Pron, and M. Zagorska, *Solid State Commun.* **67**, 471 (1988).
- ²⁵Y. W. Park, W. K. Han, C. H. Choi, and H. Shirakawa, *Phys. Rev. B* **30**, 5847 (1984).
- ²⁶J. Tsukamoto, A. Takahashi, and K. Kawasaki, *Jpn. J. Appl. Phys., Part 1* **29**, 125 (1990).
- ²⁷T. Miyamae, M. Shimizu, and J. Tanaka, *Bull. Chem. Soc. Jpn.* **67**, 2407 (1994).
- ²⁸H. H. S. Javadi, A. Chakraborty, C. Li, N. Theophilou, D. B. Swanson, A. G. MacDiarmid, and A. J. Epstein, *Phys. Rev. B* **43**, 2183 (1991).
- ²⁹Y. Nogami, H. Kaneko, H. Ito, T. Ishiguro, T. Sasaki, N. Toyota, A. Takahashi, and J. Tsukamoto, *Phys. Rev. B* **43**, 11 829 (1991).
- ³⁰A. Pron, P. Bernier, D. Billaud, and S. Lefrant, *Solid State Commun.* **46**, 587 (1983).
- ³¹D. B. Tanner, G. L. Doll, A. M. Rao, P. C. Eklund, G. A. Arbuckle, and A. G. MacDiarmid, *Synth. Met.* **28**, D141 (1989).
- ³²Y. Nogami, H. Kaneko, T. Ishiguro, A. Takahashi, J. Tsukamoto, and N. Hosoi, *Solid State Commun.* **76**, 583 (1990).
- ³³R. S. Kohlman, J. Joo, Y. Z. Wang, J. P. Pouget, H. Kaneko, T. Ishiguro, and A. J. Epstein, *Phys. Rev. Lett.* **74**, 773 (1995).
- ³⁴T. H. Gilani and T. Ishiguro, *J. Phys. Soc. Jpn.* **66**, 727 (1997).
- ³⁵R. S. Kohlman, A. Zibold, D. B. Tanner, G. G. Ihas, T. Ishiguro, Y. G. Min, A. G. MacDiarmid, and A. J. Epstein, *Phys. Rev. Lett.* **78**, 3915 (1997).
- ³⁶S. Kobayashi and F. Komori, *Prog. Theor. Phys. Suppl.* **84**, 224 (1985).
- ³⁷P. A. Lee and T. V. Ramakrishnan, *Rev. Mod. Phys.* **57**, 287 (1985).
- ³⁸T. E. Jones, W. F. Butler, T. R. Ogden, D. M. Gottfredson, and E. M. Gullikson, *J. Chem. Phys.* **88**, 3338 (1988).
- ³⁹See, for example, J. Kondo, *Solid State Phys.* **23**, 222 (1969).
- ⁴⁰J. L. Bredas, R. R. Chance, and R. Silbey, *J. Phys. Chem.* **85**, 756 (1981).
- ⁴¹H. Kaneko, T. Ishiguro, J. Tsukamoto, and A. Takahashi, *Solid State Commun.* **90**, 83 (1994).
- ⁴²A. Kurobe and H. Kamimura, *J. Phys. Soc. Jpn.* **51**, 1904 (1982).
- ⁴³T. Ishiguro, H. Kaneko, Y. Nogami, H. Ishimoto, H. Nishiyama, J. Tsukamoto, A. Takahashi, M. Yamaura, T. Hagiwara, and K. Sato, *Phys. Rev. Lett.* **69**, 660 (1992).

- ⁴⁴A. J. Epstein, H. W. Gibson, P. M. Chaikin, W. G. Clark, and G. Grüner, Phys. Rev. Lett. **45**, 1730 (1980). A $\ln T$ dependence ascribable to strong disorder was reported in this paper.
- ⁴⁵L. Cruz, P. Phillips, and A. H. Castro Neto, Europhys. Lett. **29**, 389 (1995).
- ⁴⁶R. W. Cochrane, R. Harris, J. O. Ström-Olson, and M. J. Zuckermann, Phys. Rev. Lett. **35**, 676 (1975).
- ⁴⁷A. Zawadowski and K. Vladar, in *Quantum Tunneling in Condensed Media*, edited by Yu. Kagan and A. J. Legett, Elsevier series of joint Soviet-western collection (Elsevier, Amsterdam, 1992); K. Vladar and A. Zawadowski, Phys. Rev. B **28**, 1564 (1983).
- ⁴⁸H. Kaneko, Y. Nogami, T. Ishiguro, H. Nishiyama, H. Ishimoto, A. Takahashi, and J. Tsukamoto, Synth. Met. **55-57**, 4888 (1993).